Arch. Mech., 47, 3, pp. 485–498, Warszawa 1995

# Effect of prior quasi-static loading on the initiation and growth of dynamic adiabatic shear bands (*)

R. C. BATRA (BLACKSBURG) and C. ADULLA (TROY)

WE STUDY the initiation and growth of adiabatic shear bands in a thin-walled steel tube deformed first quasi-statically either in simple compression or simple tension or by a pressure applied to the inner surface of the tube, and then by equal and opposite tangential speeds applied to the end surfaces of the tube. The objective is to see how prior quasi-static deformations of the tube affect the nominal shear strain at which a shear band initiates in the tube. The first set of numerical experiments simulates the tests recently conducted by Murphy who found that the nominal strain at the initiation of the shear bands decreased with an increase in the axial static compressive stress induced in the tube.

## 1. Introduction

ADIABATIC SHEAR BANDS are narrow regions, usually a few microns wide, of intense plastic deformation that form during high strain-rate plastic deformation of most metals. TRESCA [1] seems to be the first to observe these during the hot forging of platinum and he termed these "hot lines". Subsequently MASSEY [2] also noticed these during the hot forging process. However, the research activity in this area appears to be influenced strongly by the work of ZENER and HOLLOMON [3] who observed 32 μm wide shear bands during the punching of a hole in a steel plate. They also pointed out that the intense plastic deformations of the steel heated it up significantly, and that it became unstable when the thermal softening equalled the hardening caused by strain and strain-rate effects. The reader is referred to ROGERS [4], CLIFTON [5], OLSON *et al.* [6], and to recent issues of the Applied Mechanics Reviews [7] and the Mechanics of Materials Journal [8] for a review of the work in this area.

The experimental work under controlled conditions has been performed on tubular specimens using a Kolsky bar by DUFFY *et al.* [9, 10] and GIOVANOLA [11]. These tests have involved the twisting of a thin tube, observing deformations of a grid pasted on the outer surface of the tube and using infrared lamps to measure the temperature rise of a small region either included in or enclosing the shear band. Such observations have enhanced significantly our understanding of the mechanism of the shear band formation. Recently MURPHY [12] conducted a series of tests in which a steel tube was loaded quasi-statically in simple compression and then twisted dynamically. He found that an increase in the prior compressive load increased the nominal strain at which a shear band initiated.

(*) Paper presented at 30th Polish Solid Mechanics Conference, Zakopane, September 5–9, 1994.

Here we study the dynamic twisting of a steel tube preloaded quasi-statically either in simple compression or simple tension, or by an internal pressure. The maximum preload applied is such as not to cause plastic deformations of the tube. It is found that the nominal shear strain at which a shear band initiates increases with an increase in the value of the internal pressure, and with an increase in the tensile load applied, but decreases with an increase in the magnitude of the compressive stress. The last result contradicts test observations of MURPHY [12]. We had to increase the thickness of the tube in order to avoid its buckling. However, we observed that for the tube preloaded in either simple tension or compression, the material particles underwent significant displacements in the radial direction when the tube was twisted; these displacements were virtually zero when there was no preload applied. This change in the radial dimensions probably affects noticeably the nominal shear strain at which a shear band initiates.

## 2. Formulation of the problem

We use rectangular Cartesian coordinates and the referential description of motion to describe the dynamic deformations of an elastic-thermoviscoplastic body. The balance laws governing the deformations of a body are given, for example, in TRUESDELL and NOLL [13] and are omitted here. However, in the balance of internal energy, we assume that the deformations are locally adiabatic and that all of the plastic working rather than 90–95% of it, as asserted by FARREN and TAYLOR [14] and SULIJOADIKUSUMO and DILLON [15], is converted into heating. We note that for a thermoviscoplastic body deformed in simple shear, BATRA and KIM [16] have shown that realistic values of thermal conductivity do not affect the value of the nominal strain at which a shear band initiates. A similar result was obtained by BATRA and PENG [17] for depleted uranium and tungsten blocks deformed in plane strain compression. However, the post-localization response is influenced by heat conduction.

We make the following constitutive assumptions for the material of the tube.

(2.1) $$\sigma_{ij} = -p\delta_{ij} + s_{ij}, \qquad p = K(\varrho/\varrho_0 - 1),$$

(2.2) $$s_{ij}^{\Delta} = 2\mu(\overline{D}_{ij} - D_{ij}^p), \qquad \overline{D}_{ij} = D_{ij} - \frac{1}{3}D_{kk}\delta_{ij},$$

(2.3) $$2D_{ij} = v_{i,j} + v_{j,i}, \qquad \sigma_{ij}^{\Delta} = \dot{\sigma}_{ij} + \sigma_{ik}W_{kj} - \sigma_{jk}W_{ki},$$

(2.4) $$2W_{ij} = v_{i,j} - v_{j,i}, \qquad \varrho_0\dot{e} = \varrho c\dot{\theta} + p\frac{\dot{\varrho}}{\varrho^2}, \qquad D_{ii}^p = 0,$$

(2.5) $$D_{ij}^p = \Lambda s_{ij}, \qquad \sigma_m = (A + B(\varepsilon_p)^n)\left(1 + D\ln\left(\frac{\dot{\varepsilon}_p}{\dot{\varepsilon}_0}\right)\right)(1 - \nu\theta),$$

(2.6) $$\Lambda = 0 \quad \text{if either} \quad J_2 < \sigma_m \quad \text{or} \quad J_2 = \sigma_m \quad \text{and} \quad s_{ij}D_{ij}^p < 0,$$

otherwise, $\Lambda$ is a solution of

$$J_2 = \sigma_m, \qquad J_2 = \left(\frac{3}{2} s_{ij} s_{ij}\right)^{1/2}, \tag{2.7}$$

$$\dot{\varepsilon}_p = \left(\frac{2}{3} D^p_{ij} D^p_{ij}\right)^{1/2}, \qquad \varepsilon_p = \int \dot{\varepsilon}_p \, dt. \tag{2.8}$$

Here $\sigma_{ij}$ is the Cauchy stress tensor, $p$ the hydrostatic pressure, $\delta_{ij}$ the Kronecker delta, $K$ the bulk modulus, $\mu$ the shear modulus, a superimposed triangle indicates the Jaumann derivative, $\overline{D}_{ij}$ is the deviatoric part of the strain-rate tensor $D_{ij}$, $W_{ij}$ is the spin tensor, $q_i$ the heat flux per unit area, $c$ the specific heat and $\theta$ equals the temperature rise. Equation $(2.5)_1$ implies that the plastic strain-rate is directed along the normal to the instantaneous yield surface $J_2 = \sigma_m$, and the "radius" of the yield surface depends upon the strain-hardening, strain-rate hardening and thermal softening of the material point. The plastic strain-rate $D^p_{ij}$ equals zero when the deformations are elastic; otherwise, its value depends upon the state of deformation at the material point. The relation $(2.5)_2$ giving the dependence of $\sigma_m$ upon the plastic strain, plastic strain-rate and the temperature has been proposed by JOHNSON and COOK [18]; symbols $A$, $B$, $D$, $n$ and $\nu$ denote material parameters and $\dot{\varepsilon}_0 = 1/\text{sec}$.

We take the body to be initially stress-free, and at rest at uniform temperature $\theta_0$. It is first loaded quasi-statically and then twisted dynamically. Here the quasi-static load is simulated by applying it slowly till it reaches the desired value and subsequently holding it steady. Boundary conditions for the three loadings considered (with axial compression and tension counted as two separate loadings) are:

a. Simple compression/tension of the tube (see Fig. 1 for the choice of axes)

$$\sigma_{33}(x_1, x_2, 0, t) = -\sigma_{33}(x_1, x_2, \ell, t) = \begin{cases} \pm\sigma t/t_{rs}, & 0 \le t \le t_{rs}, \\ \pm\sigma, & t > t_{rs}, \end{cases} \tag{2.9}$$

$$\sigma_{ij}(x_1, x_2, x_3, t) n_j = 0 \tag{2.10}$$

on the inner and outer surfaces of the tube,

$$\begin{aligned} v_1(x_1, x_2, 0, t) &= \begin{cases} \varepsilon_{i3j} x_j \omega < t - t_s > /t_{rd}, & |t - t_s| \le t_{rd}, \\ \varepsilon_{i3j} x_j \omega, & (t - t_s) \ge t_{rd}, \end{cases} \\ v_i(x_1, x_2, \ell, t) &= -v_i(x_1, x_2, 0, t). \end{aligned} \tag{2.11}$$

b. Tube pressured from inside

On the inner surface of the tube

$$\begin{aligned} \sigma_{ij} n_j &= -p n_i t/t_{rs}, & 0 \le t \le t_{rs}, \\ &= -p n_i, & t \ge t_{rs}, \end{aligned} \tag{2.12}$$

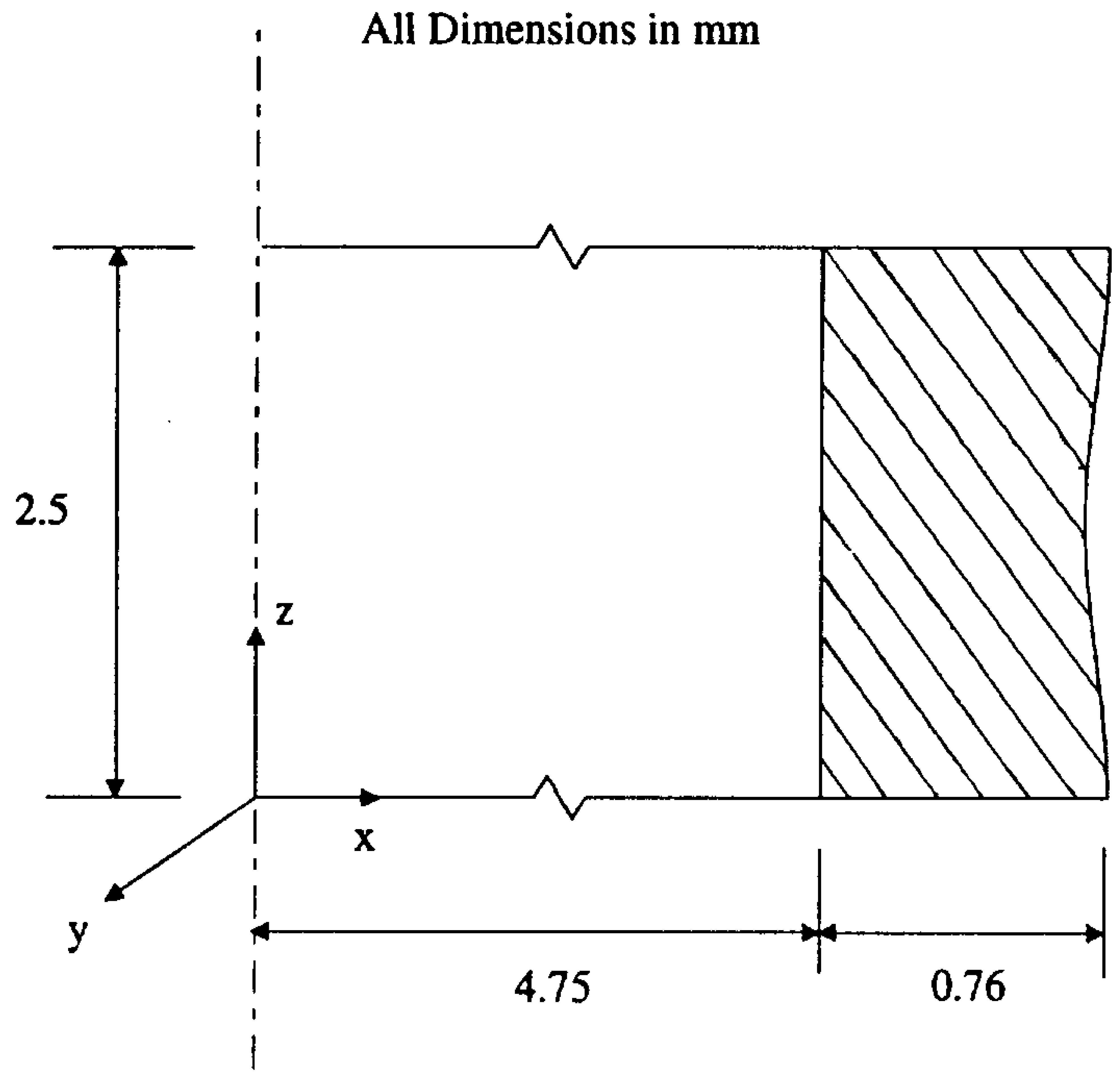


FIG. 1. Tube geometry.

and on the outer surface of the tube

$$
\begin{aligned}
\sigma_{ij}n_j &= 0, \qquad t \geq 0, \\
v_3(x_1, x_2, 0, t) &= v_3(x_1, x_2, \ell, t) = 0, \qquad 0 \leq t \leq t_s, \\
v_i(x_1, x_2, 0, t) &= \begin{cases} \varepsilon_{i3j} xj\omega < t - t_s > /t_{rd}, & |t - t_s| \leq t_{rd}, \\ \varepsilon_{i3j} x_j \omega, & (t - t_s) \geq t_{rd}, \end{cases} \\
v_i(x_1, x_2, \ell, t) &= -v_i(x_1, x_2, 0, t).
\end{aligned} \tag{2.13}
$$

That is, the tube is first loaded axially either in compression or tension from zero to an axial stress of $\sigma$ in time $t_{rs}$, the axial load is held constant for time $(t_s - t_{rs})$ so that the elastic waves can attenuate somewhat, and then the tube is twisted by applying equal and opposite tangential velocities at the ends of the tube. The angular speed increases linearly from 0 to the steady value $\omega$ in time $t_{rd}$; the quantity $< t - t_s >$ equals 0 for $t \leq t_s$, and equals $(t - t_s)$ otherwise. Equations (2.11) imply that the ends $x_3 = 0$ and $x_3 = \ell$ of the tube are subjected to equal and opposite tangential speeds. The nominal strain-rate at a point equals $2\omega r/L$, where $r$ is the radial coordinate of a point and $L$ is the initial length of the tubular specimen. Because of the small thickness of the tube, the nominal shear strain-rate varies only a little through the thickness of the tube. Henceforth, $2\omega r_m/L$ is referred to as the average shear strain-rate; $r_m$ equals the mean radius of an end-surface of the tube. The axial stress $\sigma$ and the internal pressure $p$ are limited to a small fraction of the yield stress of the material. Thus the preload causes only elastic deformations of the tube. In Eqs. (2.11) and (2.13), $\varepsilon_{ijk}$ is the permutation symbol and equals 1 or $-1$ accordingly as $i$, $j$, $k$ form an even or an odd permutation of 1, 2, and 3; and equals 0 when any two indices are equal. Even though the pressure applied to the inner surface of the tube equals a fraction of the yield stress of the material, the state of stress at a point is biaxial and some material points may yield.

## 3. Results and discussion

In order to compute numerical results, we assigned following values to various material and geometric parameters.

$$\varrho = 7860\,\mathrm{kg/m^3}, \qquad G = 76\,\mathrm{GPa}, \qquad \theta_m = 1520°\,\mathrm{C},$$

$$c = 473\,\mathrm{J/kg°\,C}, \qquad \theta_0 = 25°\,\mathrm{C}, \qquad A = 792.2\,\mathrm{MPa},$$

$$B = 509.5\,\mathrm{MPa}, \qquad D = 0.014, \qquad n = 0.26, \qquad m = 1.03,$$

maximum tube thickness = 0.76 mm, inner radius of the tube = 4.75 mm, $L$ = 2.5 mm,

$$t_{rs} = 20\,\mu\mathrm{s}, \qquad t_s = 50\,\mu\mathrm{s}, \qquad t_{rd} = 20\,\mu\mathrm{s}. \tag{3.1}$$

The values of material parameters taken from RAJENDRAN'S report [18] are for 4340 steel. The thickness of the tube was assumed to vary sinusoidally:

$$\frac{w(x_3)}{w_A} = 1 + \frac{\varepsilon}{2}\left(\cos\frac{2\pi x_3}{L} - 1\right), \tag{3.2}$$

where $\varepsilon$ can be viewed as the defect parameter, $w(x_3)$ is the wall thickness at a point $x_3$ along the gage section, $w_A$ is the maximum wall thickness, and $L$ is the initial length of the tube; the thickness variation given by Eq. (3.2) is depicted in Fig. 1 for $\varepsilon = 0.08$. The thickness of the tubular specimens employed by MURPHY [12] was also given by Eq. (3.2). However, the value of $w_A$ in our simulations is twice that used by Murphy, since computations with the tube employed by Murphy indicated buckling of the tube prior to the initiation of a shear band. Also, the tubes tested by Murphy were made of HY-100 steel but parameters given in (3.1) are for a 4340 steel. It is because values of material parameters for HY-100 steel for the Johnson-Cook model are not available. Also, there are not enough test data available for HY-100 steel to determine the values of $A$, $B$, $D$ etc. for it. We should note that because of the nonlinearities involved, the determination of material parameters from the test data is not unique.

The problems formulated in the previous section were solved numerically by using the large scale explicit finite element code DYNA3D [19]. The code uses

8-noded brick elements with one-point quadrature rule to evaluate various integrals. It employs hour-glass control to eliminate the spurious modes and artificial viscosity to smear out the shocks. The time step size is computed suitably so as to satisfy the Courant condition, thereby ensuring the stability of the computed solution.

Even though the specimen geometry and the loading conditions are such as to cause axisymmetric deformations of the tube, the problem is solved as three-dimensional because of the way the boundary conditions are applied in the code. Also antisymmetry of the velocity field about the midplane suggests that deformations of only half of the tube should be studied. Since the code DYNA3D employs Cartesian coordinates, the imposition of the constraint that points on the midplane move only radially required a major modification of the code. It was done and accordingly deformations of the entire tube were analyzed.

In order to assess the effect of the finite element mesh on the solution of the problem, two different meshes were tried, one containing nearly four times the number of elements as the other; these are depicted in the insert of Fig. 2. It

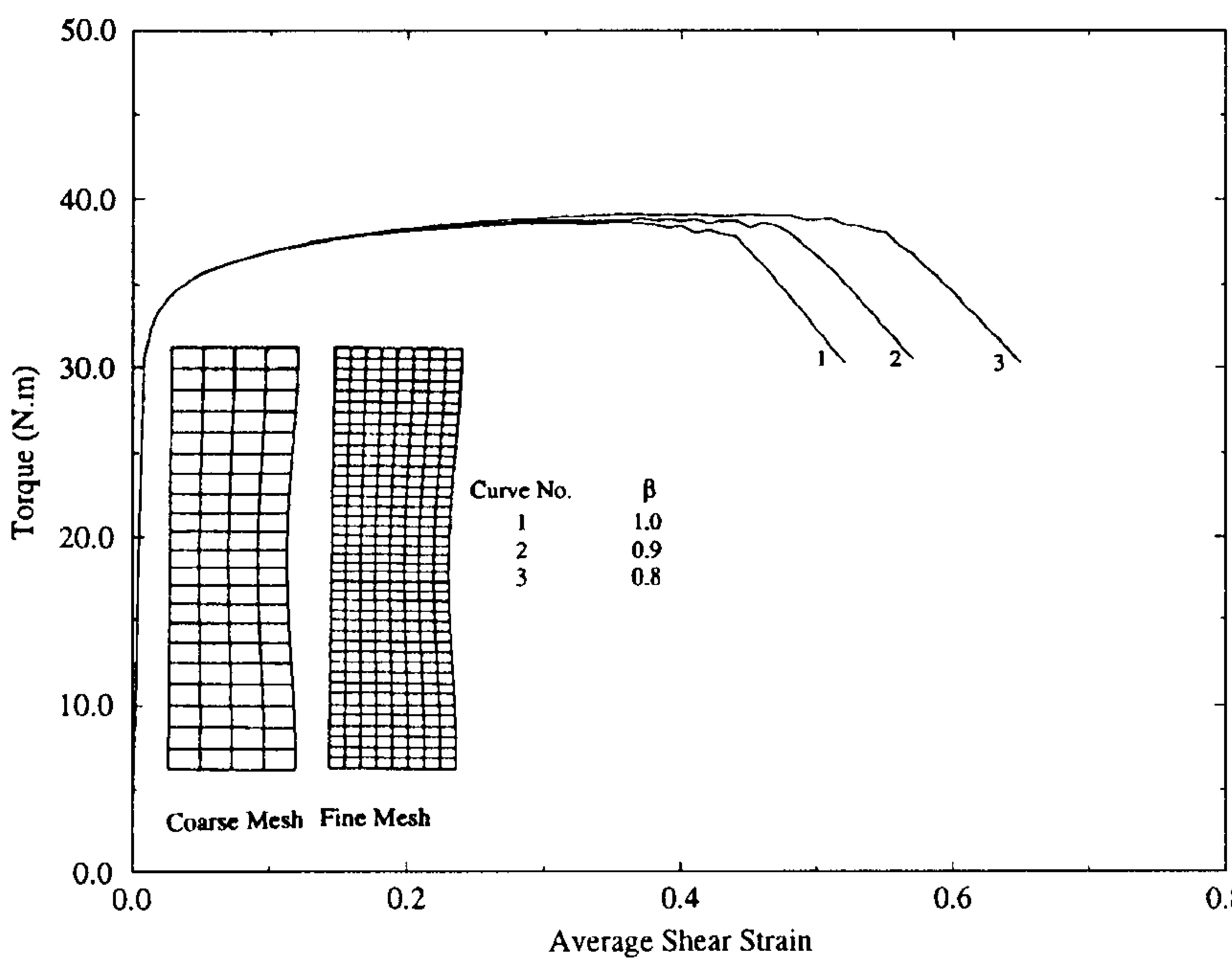


FIG. 2. Torque vs. average shear strain curves for three different values of the fraction $\beta$ of plastic work converted into heat. The insert shows the coarse and fine meshes used.

was found that the torque required to deform the tube versus the average shear strain curve was unaffected by the mesh used. However, the rate of drop of the torque is considerably more for the fine mesh as compared to that for the coarse mesh, since once a shear band initiates, the fine mesh is capable of delineating the sharp gradients of the deformation fields better than the coarse mesh. Also, the axisymmetric deformations are essentially concentrated in one central row of elements which, for the fine mesh, is of smaller size. The CPU time required to analyze the problem with the fine mesh is nearly 4 times that required for the coarse mesh. Thus, if the objective is to find the value of the nominal shear strain when a shear band initiates, it is sufficient to use a coarse mesh.

In DYNA3D artificial bulk viscosity is added to smear out the shocks. One of its consequences can be that the initiation of a shear band is either delayed or is totally suppressed. In applying the artificial viscosity method, the pressure in elements being compressed is augmented by an artificial viscous term, $q$, before evaluating the stress divergence. In expanding elements $q = 0$, otherwise

$$q = \varrho\hat{\ell}|D_{kk}(|Q_1\hat{\ell}|D_{kk}| + Q_2\hat{c}), \tag{3.3}$$

where $Q_1$ and $Q_2$ are dimensionless constants which default to 1.5 and 0.06, respectively, $\hat{\ell}$ is the cube root of the volume of the element, and $\hat{c}$ is the speed of sound in the material and equals $((K + (4/3)G)/\varrho_0)^{1/2}$. For a fixed mesh, we computed results for $Q_1 = 1.0$, 1.25 and 1.5, and for each value of $Q_1$, $Q_2$ was assigned values 0.02, 0.04 and 0.06. The time-history of the torque required to deform the tube was found to be virtually identical for the nine cases signifying that the average shear strain at which a shear band initiates is unaffected by the value of the artificial viscosity. Results presented below are for $Q_1 = 1.5$ and $Q_2 = 0.06$.

### 3.1. Effect of the fraction of plastic work converted into heat

Because the deformations have been assumed to be locally adiabatic, i.e., the effect of heat conduction has been neglected, the temperatue rise at a material point is directly proportional to the total plastic work done there. A lower fraction, $\beta$, of the plastic work converted into heat will delay the rise in the temperature of a material particle and hence, the shear band will initiate at a higher value of the average strain. That this indeed is the case is clear from the torque versus the average shear strain curves depicted in Fig. 2 for the three cases, namely, when 100%, 90%, or 80% of the plastic work is converted into heat. Because of the nonlinearities in the problem, the incremental changes in the value of the average shear strain are unequal for the same incremental changes in the value of $\beta$. Henceforth, we assume that all of the plastic work is converted into heat.

### 3.2. Effect of initial axial load

For the case when the tube is first axially loaded quasi-statically either in compression or in tension and then twisted with the load curves defined by Eq. (2.11), Figs. 3 and 4 illustrate the torque versus average shear strain curves for four different values of the axial load. Note that the maximum axial stress applied equals 45% of the value of the material parameters $A$ appearing in Eq. (2.5). Because of the prestress, the shear stress and hence the torque required to initiate yielding

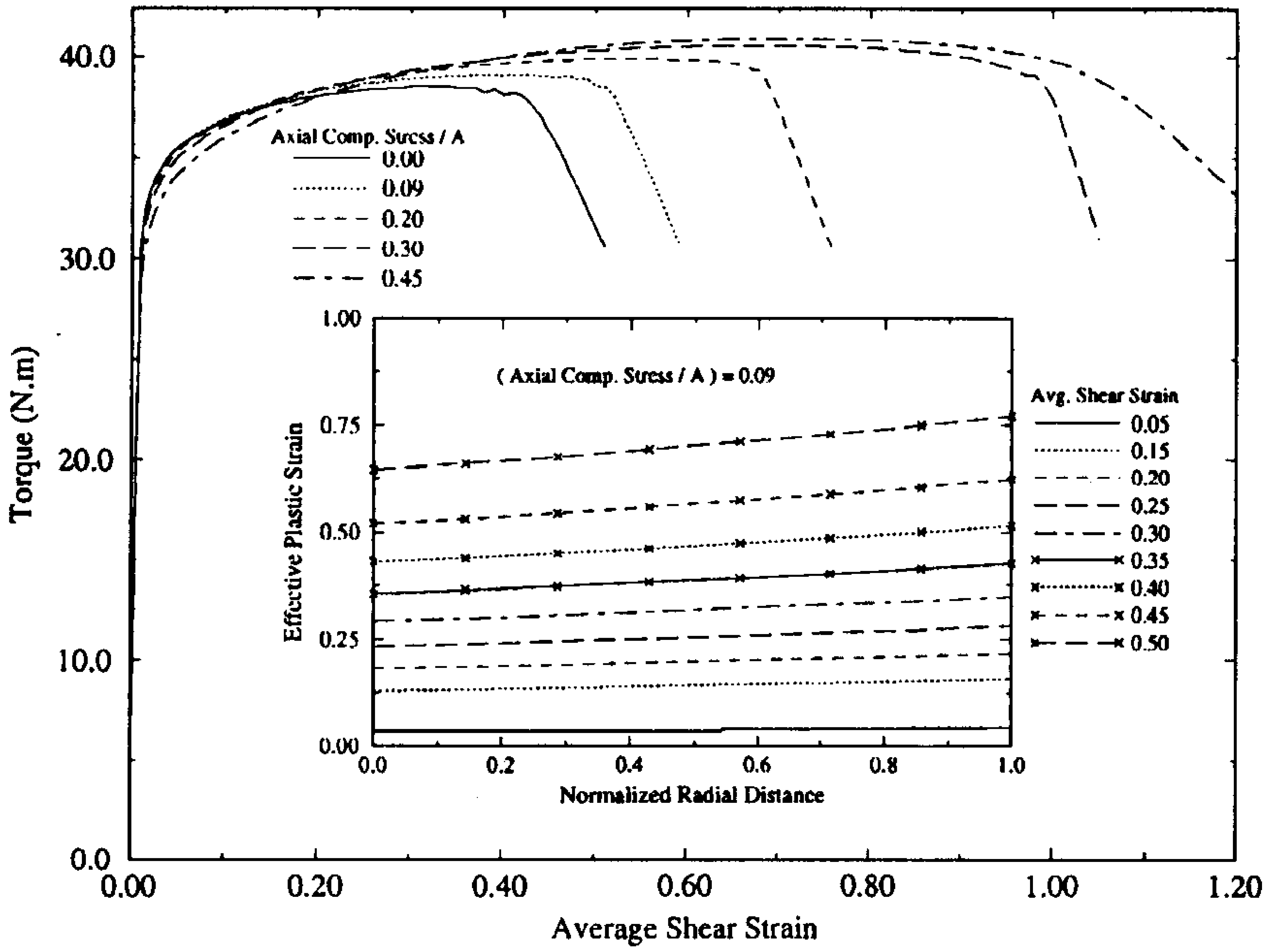


FIG. 3. Torque vs. average shear strain curves for five different values of the initial axial compressive stress. The insert shows the distribution of the effective plastic strain, at different times, on a radial line in the thinnest cross-section.

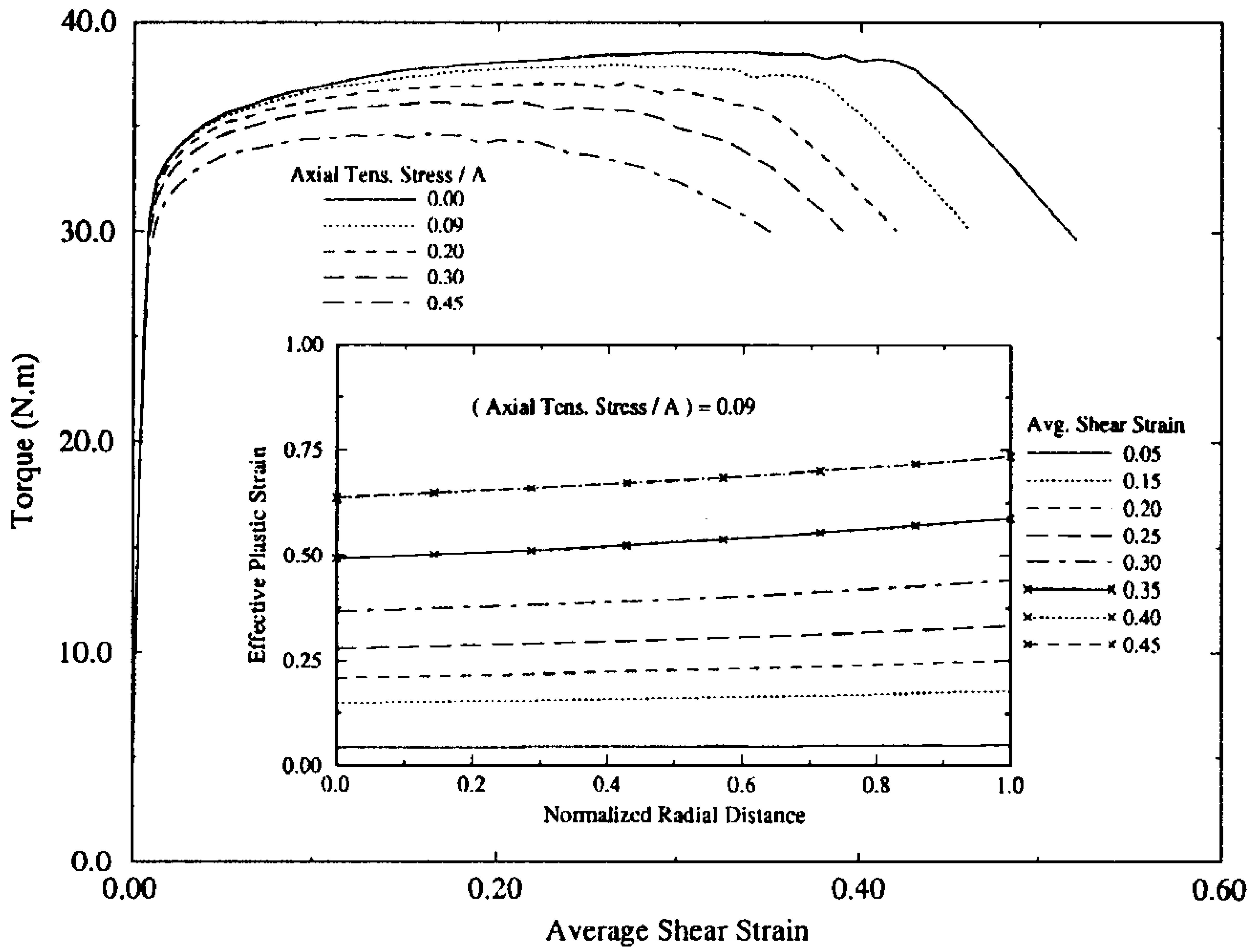


FIG. 4. Torque vs. average shear strain curves for four different values of the initial axial tensile stress. The insert depicts the distribution of the effective plastic strain, at different times, on a radial line in the thinnest cross-section.

should be less than that necessary when there is no prestress applied. Results plotted in Figs. 2 and 3 confirm this. The average shear strain at which a shear band initiates, as indicated by the drop in the torque required to deform the tube, increases with an increase in the magnitude of the axial compressive prestress and the reverse happens when the prestress is tensile. This trend contradicts the experimental observations of MURPHY [12] who reported that the average shear strain at the instant of the initiation of a shear band decreased with an increase in the magnitude of the axial compressive prestress. A close examination of the deformed shape of the tube indicated significant radial displacements of points on the central cross-section; for example, see Fig. 5. The inserts in Figs. 3 and 4 depict distribution of the effective plastic strain on a radial line in the thinnest section of the tube. It is clear that deformations of the tube along the radial line are nonhomogeneous, with the largest effective plastic strain occurring at points on the outermost surface of the tube. For axial prestress equal to $0.09A$, the shear band initiates at average shear strains of 0.48 and 0.37 for the compressive and tensile cases; however, the distribution of the effective plastic strain along the radial direction is essentially the same in the two cases. The severe deformations of the central cross-section result in an increase of the cross-sectional area for tubes prestressed in compression, and in a decrease of the cross-sectional area for tubes preloaded in tension. This change in the cross-sectional area delays the initiation of the shear band for the tube prestressed in compression and enhances the initiation of the shear band in the tube prestressed in tension. We note that the axial length of the tube decreases (increases) for the tube prestressed in compression (tension). It is not clear whether Murphy's experimental set-up allowed for this change in the axial length of the specimen. For the case of no preload, the tube length, the inner radius, and the outer radius remained unchanged.

We simulated a case when one end of the tube was held fixed and at the other end the axial component of velocity was first increased linearly from zero to the desired value in $20\mu s$, so as to induce an axial compressive stress in the tube by the desired amount. Subsequently, the axial component of velocity was decreased to zero and a tangential component of velocity was prescribed. This type of boundary data resulted in a gradual decrease of the axial compressive stress to zero. Analysis of the quasi-static problem involving a cylinder subjected to compressive and torsional loads given in CHAKRABARTY'S book [20] suggests that this trend is consistent with the predictions of the Prandtl-Reuss theory of plasticity.

Figure 6 depicts the evolution of the effective plastic strain on an axial line on the outer surface of the tube obtained by using a fine mesh. It is evident that deformations are nonhomogeneous even at an average shear strain of 0.05, and this nonhomogeneity in the deformations increases as the tube continues to be twisted. Eventually the deformations localize in the central element. Once it happens, the material outside this element does not undergo any more plastic deformations, and some parts may even unload. The width of the region of localization cannot be deciphered accurately since the mesh used is not fine enough.

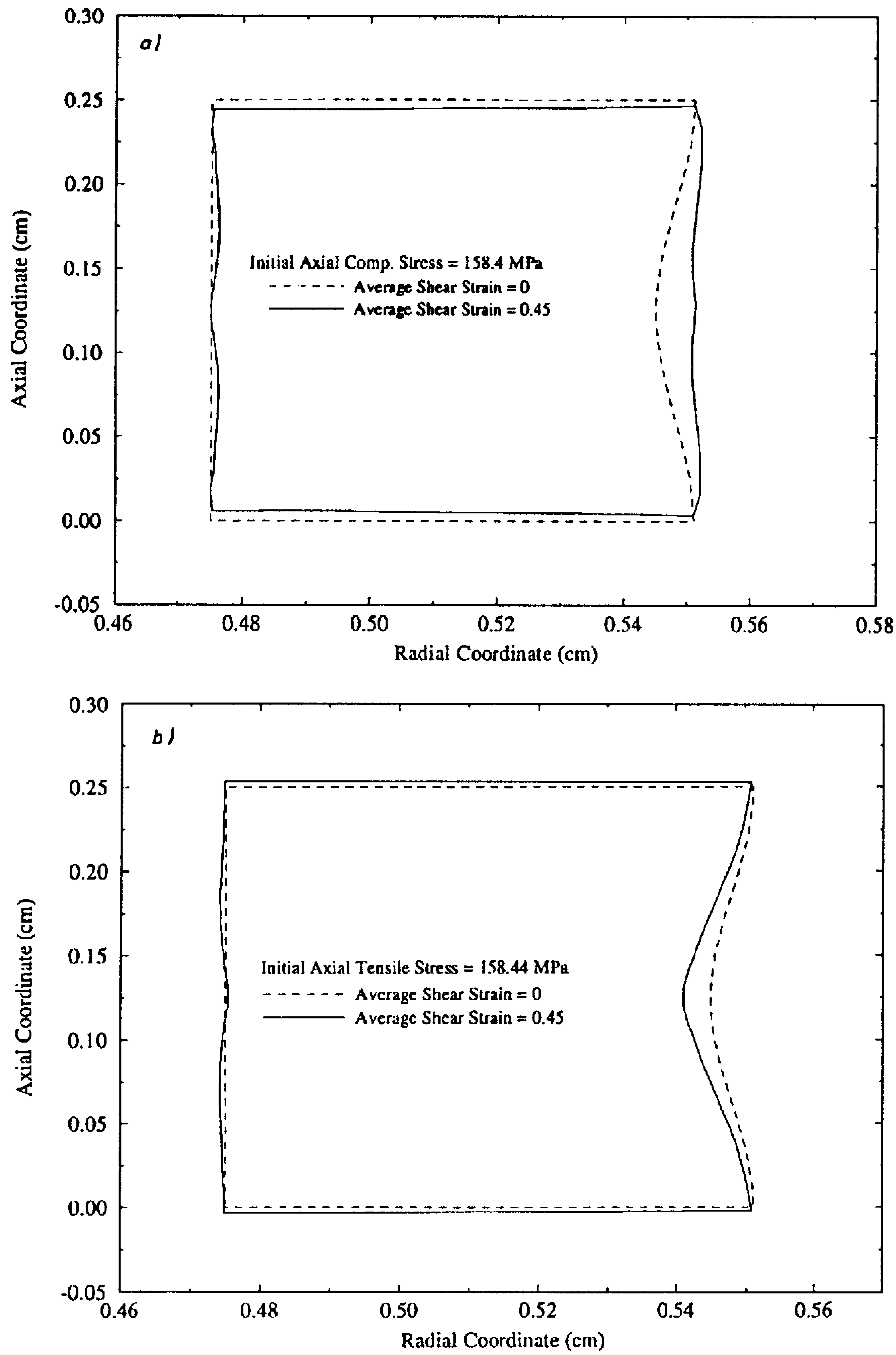


FIG. 5. Sections of the deformed tubes initially prestressed in (a) compression and (b) tension.

For this reason, the computations were stopped soon after the torque required to deform the tube began to drop. We note that in the code effective plastic strains are computed at the centroids of the elements.

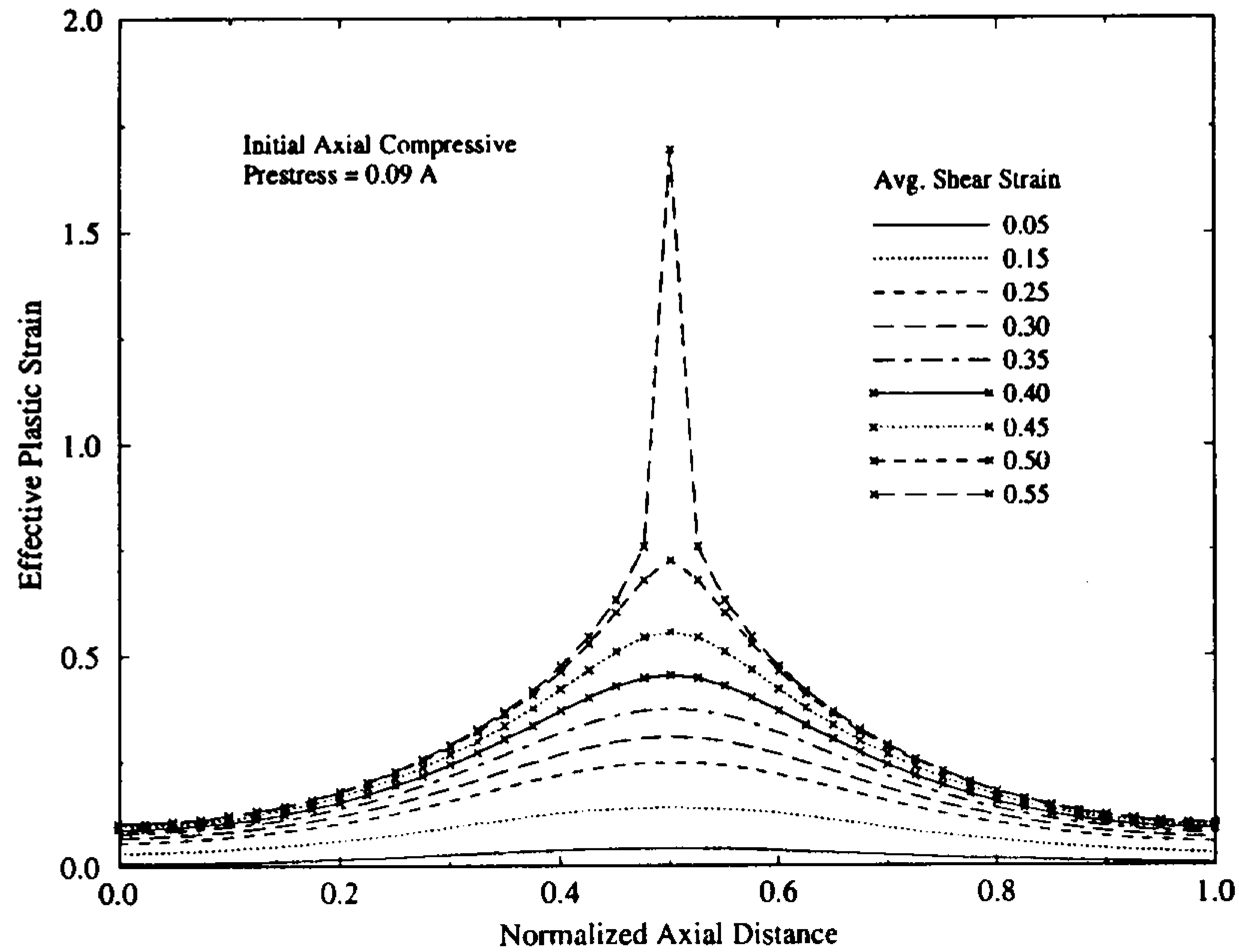


FIG. 6. Distribution of the effective plastic strain at different times on a line parallel to the axis of the tube and passing through the outermost point of the thinnest cross-section.

### 3.3. Effect of initial internal pressure

We assume that the end surfaces are held fixed in the axial direction and an internal pressure is applied slowly to the tubular specimen. Even when the internal pressure applied was 71.3 MPa, the stress state at a point was such as to cause no yielding of the material. Subsequently, with the internal pressure held steady, the end surfaces are twisted in equal and opposite directions by applying tangential velocity on them so as to induce an average shear strain-rate of $5000\,s^{-1}$. In Fig. 7 we have plotted the torque required to deform the tube versus the average shear strain. As expected, with an increase of the internal pressure the shear stress and hence the torque when the tube begins to deform, plastically decrease. However, the average shear strain at which a shear band initiates increases with an increase in the value of the internal pressure because of an increase in the inner and outer radii of the tube. Figure 8 illustrates the distribution, on a radial line, of the effective plastic strain at different times. Whereas initially the effective plastic strain is a little higher at points on the outermost surface than that at points on the innermost surface, the reverse happens after the shear band has initiated. Also, the variation of the effective plastic strain in the radial direction is not linear as was the case for the tube prestressed in axial tension or compression. Figure 9 depicts a longitudinal section of the tube just before the torque is applied and also when the average strain equals 0.45. It is clear that significant radial displacements of material points occur during the time the tube is being twisted.

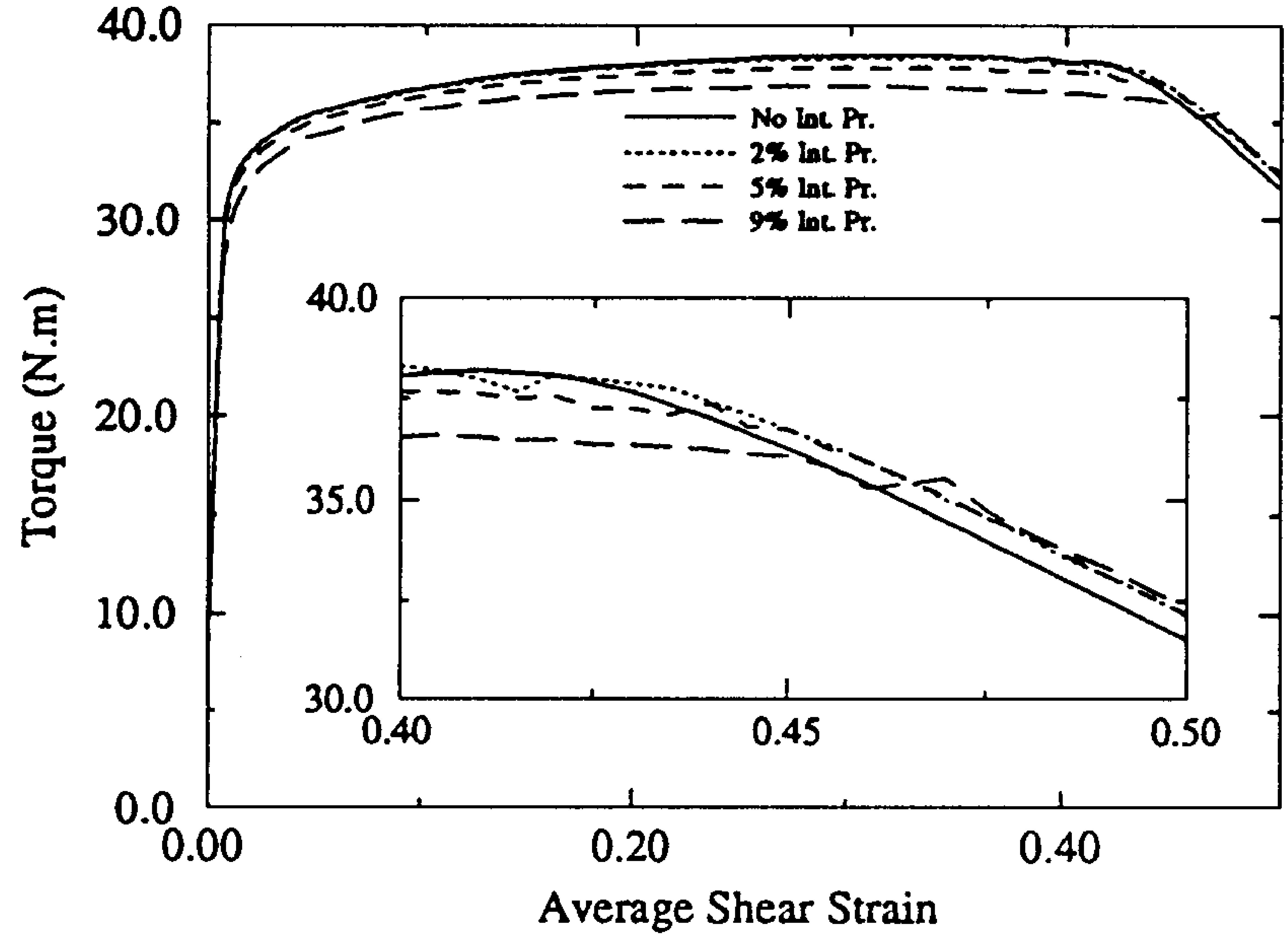


FIG. 7. Torque vs. average shear strain curves for four different values of the internal pressure.

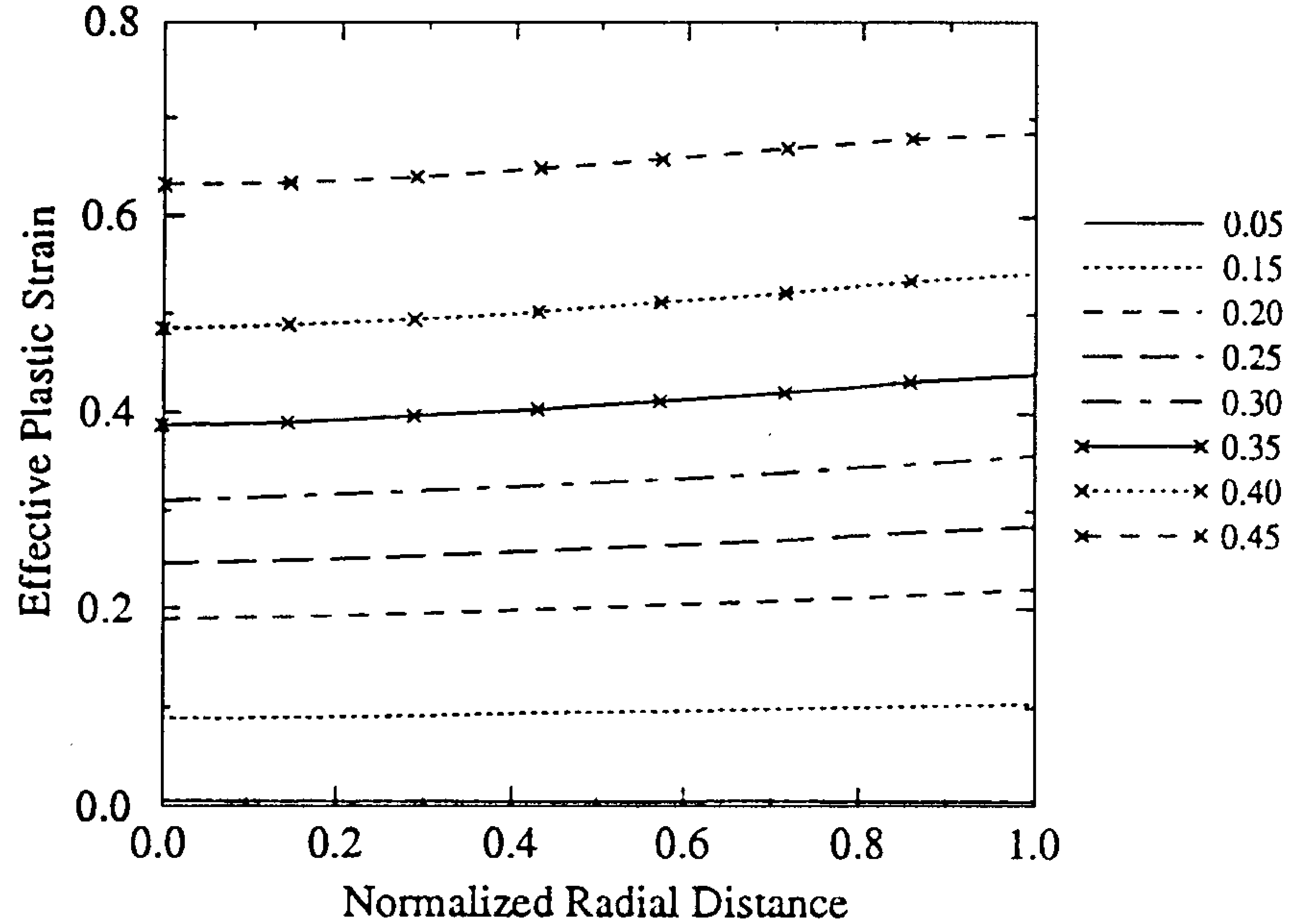


FIG. 8. The distribution of effective plastic strain, at different times, on a radial line in the thinnest cross-section.

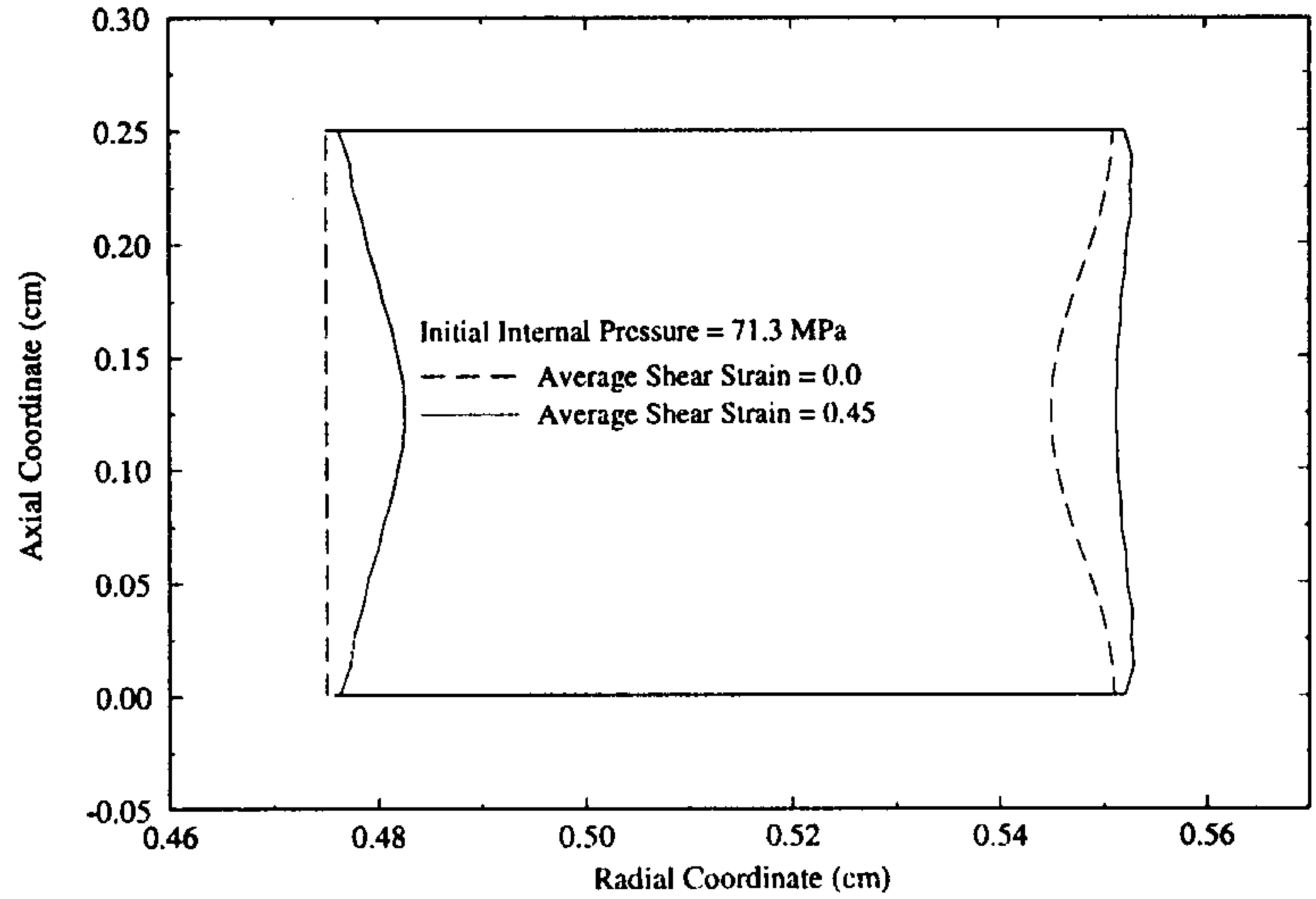


FIG. 9. A longitudinal section of the deformed tube.

## 4. Conclusions

We have studied the effects of the prior axial load and internal pressure applied quasi-statically on tubular specimens which are subsequently deformed dynamically in torsion. The thickness of the tube varies sinusoidally. It is accomplished by keeping the inner radius fixed but varying the outer radius, so as to obtain minimum thickness at the central cross-section of the tube. The thermomechanical response of the material of the tube is modeled by the Johnson-Cook law. For a tube with no preload, the inner radius and the axial length of the tube remained unchanged during its torsional deformations. However, for a preloaded tube, these dimensions changed noticeably. The average shear strain, $\gamma_c$, at the instant of the initiation of the shear band, as signified by a sudden drop in the torque required to deform the tube, is found to increase with an increase in the magnitude of the axial compressive stress or the internal pressure, and decrease with an increase in the value of the tensile stress. The main reason for the difference in the response of the tube prestressed in compression and tension is due to the deformations of the central section of the tube.

## 5. Acknowledgements

This work was supported by the U.S. National Science Foundation grant CMS9411383 to the Virginia Polytechnic Institute and State University. Some of the computations were performed on the NSF sponsored supercomputer center at the Cornell University, Ithaca, NY.

## References


1. H. TRESCA, *On further application of the flow of solids*, Proc. Inst. Mech. Engng., **30**, 301–345, 1878.
2. H.F. MASSEY, *The flow of metal during forging*, Proc. Manchester Assoc. Engng., 21–26, 1926.
3. C. ZENER and J.H. HOLLOMON, *Effect of strain rate on plastic flow of steel*, J. Appl. Phys., **14**, 22–32, 1944.
4. H.C. ROGERS, *Adiabatic plastic deformation*, Ann. Rev. Mat. Sci., 299–311, 1979.
5. R.J. CLIFTON, *Adiabatic shear banding*, Material Response to Ultra-High Loading Rates, NRC Report NMAB-356, 129–142, 1980.
6. G.B. OLSON, J.F. MESCALL and M. AZRIN, *Adiabatic deformation and strain localization*, [in:] Shock Waves and High Strain-Rate Phenomenon in Metals, M.A. MEYERS and L.E. MURR [Eds.], Plenum Press, NY, 221–247, 1980.
7. H.M. ZBIB, T. SHAWKI and R.C. BATRA [Eds.], *Material Instabilities*, Special Issue of Applied Mechanics Reviews, **45**, 3, March 1992.
8. R.C. ARMSTRONG, R.C. BATRA, M.A. MEYERS and T.W. WRIGHT [guest editors], *Special Issue on Shear Instabilities and Viscoplasticity Theories*, Mech. Materials, **17**, 83–327, 1994.
9. K.A. HARTLEY, J. DUFFY and R.H. HAWLEY, *Measurement of the temperature profile during shear band formation in steels deforming at high strain rates*, J. Mech. Phys. Solids, **35**, 283–301, 1987.
10. A. MARCHAND and J. DUFFY, *An experimental study of the formation process of adiabatic shear bands in a structural steel*, J. Mech. Phys. Solids, **36**, 251–283, 1988.
11. J.H. GIOVANOLA, *Adiabatic shear banding under pure shear loading. Part I. Direct observation of strain localization and energy dissipation measurements*, Mech. Materials, **7**, 59–72, 1988.
12. B.P. MURPHY, *Shear band formation in a structural steel under a combined state of stress*, M. Sc. Thesis, Brown University, Providence 1990.
13. C.A. TRUESDELL and W. NOLL, *Nonlinear field theories of mechanics*, Handbuch der Physik, III/3, S. FLÜGGE [Ed.], Springer Verlag, Berlin 1965.
14. W.S. FARREN and G.I. TAYLOR, *The heat developed during plastic extrusion of metal*, Proc. Roy. Soc., **A107**, 422, 1925.
15. A.U. SULIJOADIKUSUMO and O.W. DILLON, Jr., *Temperature distribution for steady axisymmetric extrusion with an application to Ti-6Al-4V. Part 1*, J. Thermal Stresses, **2**, 97–112, 1979.
16. R.C. BATRA and C.H. KIM, *Effect of heat conduction on the initation and growth of shear bands*, Int. J. Engng. Sci., **29**, 949–960, 1991.
17. R.C. BATRA and Z. PENG, *Development of shear bands in dynamic plane strain compression of depleted uranium and tungsten blocks*, Int. J. Impact Engng., 1995 [to appear].
18. G.R. JOHNSON and W.H. COOK, *Constiutive model and data for metals subjected to large strains, high strain rates and high temperatures*, Proc. 7th Int. Symp. Ballistics, pp. 541–548, The Hague, The Netherlands 1983.
19. A.M. RAJENDRAN, *High strain rate behavior of metals, ceramics and concrete*, Report # WL-TR-92-4006, Wright Patterson Air Force Base, 1992.
20. R.G. WHIRLEY and J.O. HALLQUIST, *DYNA3D user's manual (A nonlinear "Explicit", three-dimensional finite element code for solid and structural mechanics)*, UCRL-MA-107254, Univ. California, Lawrence Livermore National Laboratory, 1991.
21. J. CHAKRABARTY, *Theory of plasticity*, McGraw Hill Book Co., 1987.


DEPARTMENT OF ENGINEERING SCIENCE AND MECHANICS
VIRGINIA POLYTECHNIC INSTITUTE AND STATE UNIVERSITY, BLACKSBURG, USA.

*Received February* 27, 1995.